



# Postnatal Development of Centrifugal Inputs to the Olfactory Bulb

Johanna K. Kostka and Sebastian H. Bitzenhofer\*

*Institute of Developmental Neurophysiology, Center for Molecular Neurobiology, University Medical Center Hamburg-Eppendorf, Hamburg, Germany*

## OPEN ACCESS

### Edited by:

Friedrich Wilhelm Johanning,  
Charité Universitätsmedizin Berlin,  
Germany

### Reviewed by:

Matt Wachowiak,  
The University of Utah, United States  
Thomas Heinbockel,  
Howard University, United States

### \*Correspondence:

Sebastian H. Bitzenhofer  
sebastian.bitzenhofer@  
zmnh.uni-hamburg.de

### Specialty section:

This article was submitted to  
Neurodevelopment,  
a section of the journal  
Frontiers in Neuroscience

**Received:** 15 November 2021

**Accepted:** 07 February 2022

**Published:** 24 February 2022

### Citation:

Kostka JK and Bitzenhofer SH  
(2022) Postnatal Development  
of Centrifugal Inputs to the Olfactory  
Bulb. *Front. Neurosci.* 16:815282.  
doi: 10.3389/fnins.2022.815282

Processing in primary sensory areas is influenced by centrifugal inputs from higher brain areas, providing information about behavioral state, attention, or context. Activity in the olfactory bulb (OB), the first central processing stage of olfactory information, is dynamically modulated by direct projections from a variety of areas in adult mice. Despite the early onset of olfactory sensation compared to other senses, the development of centrifugal inputs to the OB remains largely unknown. Using retrograde tracing across development, we show that centrifugal projections to the OB are established during the postnatal period in an area-specific manner. While feedback projections from the piriform cortex (PIR) are already present shortly after birth, they strongly increase in number during postnatal development with an anterior-posterior gradient. Contralateral projections from the anterior olfactory nucleus (AON) are present at birth but only appeared postnatally for the nucleus of the lateral olfactory tract (nLOT). Numbers of OB projecting neurons from the lateral entorhinal cortex (LEC), ventral hippocampus, and cortical amygdala (CoA) show a sudden increase at the beginning of the second postnatal week and a delayed development compared to more anterior areas. These anatomical data suggest that limited top-down influence on odor processing in the OB may be present at birth, but strongly increases during postnatal development and is only fully established later in life.

**Keywords:** olfaction, olfactory bulb, centrifugal, feedback, development, postnatal, glutamatergic

## INTRODUCTION

Sensory inputs are a strong driver of neuronal activity in early sensory areas, but sensory processing is not a strict feedforward process. Centrifugal inputs from downstream areas provide information about contextual factors, such as behavioral state, attention, or prior knowledge, that strongly modulate early sensory activity (Gilbert and Sigman, 2007). However, little is known about the development of centrifugal projections.

The development of centrifugal projections to the olfactory bulb (OB) is of particular interest because newborn rodents rely on olfaction for their survival when most other senses are still non-functional (Sullivan, 2003; Logan et al., 2012). Odor processing begins with the binding of odor molecules to olfactory receptors on olfactory receptor neurons (ORNs) in the olfactory epithelium. ORNs send direct projections to structures called glomeruli in the OB, the first central processing stage for olfactory information. In the glomeruli, ORNs synapse onto dendrites of mitral and tufted

cells, the principal cells in the OB, that transmit olfactory information to a range of brain areas, including the anterior olfactory nucleus (AON), piriform cortex (PIR), olfactory tubercle, nucleus of the lateral olfactory tract (nLOT), cortical amygdala (CoA), and lateral entorhinal cortex (LEC) (Igarashi et al., 2012). In the adult brain, most of these areas, with exception of the olfactory tubercle, send glutamatergic feedback projections to the OB, providing fast top-down modulation of olfactory processing (Luskin and Price, 1983; Shipley and Adamek, 1984; In 't Zandt et al., 2019; Padmanabhan et al., 2019). Additionally, glutamatergic feedback from CA1 of the ventral hippocampus to the OB has been described in adult mice (Padmanabhan et al., 2019).

The adult OB also receives inputs from neuromodulatory areas, such as noradrenergic, serotonergic, and cholinergic input (Brunert and Rothermel, 2021). While noradrenergic inputs are well developed at birth in rodents (McLean and Shipley, 1991), serotonergic and cholinergic inputs mainly form postnatally (McLean and Shipley, 1987; Le Jeune and Jourdan, 1991).

In adults, glutamatergic centrifugal projections to the OB mainly target inhibitory neurons in the glomerular layer and granule cell layer and are thereby ideally positioned to modulate network activity (Boyd et al., 2012; Markopoulos et al., 2012). Centrifugal inputs to OB provide diverse feedback critical for the formation of odor-reward associations (Kiselycznyk et al., 2006; Gao and Strowbridge, 2009; Markopoulos et al., 2012; Boyd et al., 2015). The ability of rodents to form odor-reward associations early in life suggests that feedback projections to the OB may be established early during development (Logan et al., 2012). While feedforward projections from the OB are established at birth (Walz et al., 2006) and OB activity drives downstream areas early in life (Gretenkord et al., 2019; Kostka et al., 2020; Kostka and Hanganu-Opatz, 2021), the development of glutamatergic centrifugal projections to the OB is largely unknown. We took advantage of retrograde virus-labeling to investigate the maturation of glutamatergic centrifugal inputs to the main OB during postnatal development in mice.

## MATERIALS AND METHODS

### Animals

All experiments were performed in compliance with the German laws and the guidelines of the European Union for the use of animals in research (European Union Directive 2010/63/EU) and were approved by the local ethical committee (Behörde für Gesundheit und Verbraucherschutz Hamburg, ID 15/17).

Experiments were carried out in C57BL/6J mice of both sexes. Timed-pregnant mice from the animal facility of the University Medical Center Hamburg-Eppendorf were housed individually at a 12 h light/12 h dark cycle and were given access to water and food *ad libitum*. The day of birth was considered postnatal day (P) 0.

### Virus Injections

For retrograde labeling of OB-projecting neurons, C57BL/6J mice received unilateral injections of AAVrg-CaMKII $\alpha$ -mCherry

(200 nl at 200 nl/min, titer  $2 \times 10^{13}$  vg/ml, #114469-AAVrg, Addgene, Watertown, MA, United States) into the right main OB (0.5 mm lateral from midline, 0.5 mm rostral to the inferior cerebral vein, 0.5–1.0 mm deep). Injections were performed at P0, P3, P6, P9, P12, or P49 in a stereotaxic apparatus using a micropump (Micro4, WPI, Sarasota, FL, United States) under anesthesia. Following injection, the syringe was left in place for >60 s to reduce reflux. Mice were kept on a heating blanket until full recovery from anesthesia and returned to their home cage.

In total, 9 days after virus injection, mice were transcardially perfused with 4% paraformaldehyde (PFA). Brains were removed, post fixed in PFA for 24–48 h, and stored in phosphate buffered saline (PBS) with 0.02 sodium azide. Brains were sliced into coronal sections at 100  $\mu$ m and mounted with Vectashield with DAPI (Vector Laboratories, Burlingame, CA, United States). Fluorescence images were taken to validate injection sites and to identify areas with retrogradely labeled neurons.

### Retrobead Injections

For retrograde labeling of OB-projecting neurons, C57BL/6J mice received unilateral injections of Red Retrobeads (300 nl at 200 nl/min, Lumafluor Inc., Durham, NC, United States) into the right OB (0.5 mm lateral from midline, 0.5 mm rostral to the inferior cerebral vein, 0.5–1.0 mm deep). Injections were performed at P0, P6, or P12 in a stereotaxic apparatus using a micropump (Micro4, WPI, Sarasota, FL, United States) under anesthesia. Following injection, the syringe was left in place for >120 s to reduce reflux. Mice were kept on a heating blanket until full recovery from anesthesia and returned to their home cage.

In total, 3 days after Retrobead injection, mice were transcardially perfused with 4% paraformaldehyde (PFA). Brains were removed, post fixed in PFA for 24–48 h, and stored in phosphate buffered saline (PBS) with 0.02 sodium azide. Brains were sliced into coronal sections at 100  $\mu$ m and mounted with Vectashield with DAPI (Vector Laboratories, Burlingame, CA, United States). Fluorescence images were taken to validate injection sites.

### Cell Quantification

Single images ( $2,048 \times 2,048$  pixels) were taken with a confocal microscope (Zeiss, Oberkochen, Germany) using a 20 $\times$  objective with a 405 nm laser for DAPI and a 568 nm laser for mCherry. This resulted in a pixel size of  $0.156 \times 0.156$   $\mu$ m, corresponding to images of  $319.5 \times 319.5$   $\mu$ m. Brain areas were identified according to the Mouse reference atlas from Allen brain atlas (Lein et al., 2007). Cells were detected with Cellpose (Stringer et al., 2021), a deep learning-based cellular segmentation algorithm in Python 3.8. Parameters were kept constant for all images and results were validated by visual inspection. DAPI labeled cell bodies were counted manually with ImageJ. Retrobead labeling was detected as percent of pixels in the red channel above a threshold set depending on the background staining in the image. Data were imported and analyzed in Matlab R2021a. Data are shown as mean  $\pm$  standard error of the mean (SEM). One-way ANOVAs

followed by *post-hoc* comparisons with Tukey-Kramer correction for multiple comparisons were performed to statistically test for changes across age.

## RESULTS

### Retrograde Labeling of Olfactory Bulb-Projecting Neurons Across Development

To investigate the development of centrifugal projections to the OB, we injected AAVrg-CaMKII $\alpha$ -mCherry in the right OB of P0 ( $n = 3$ ), P3 ( $n = 2$ ), P6 ( $n = 2$ ), P9 ( $n = 6$ ), P12 ( $n = 5$ ), or P49 ( $n = 4$ ) mice to transduce neurons with axons projecting to the injection area at the day of injection (Figure 1A). P49 mice were considered adult since we did not assume further changes in OB-feedback projections at that age. Mice were perfused 9 days after injection to allow for the expression of the plasmid. Injection

areas were confirmed post-mortem (Figures 1B,C). Although injection areas in the main OB were carefully inspected, due to the retrograde labeling of neurons in nearby areas we cannot rule out completely that some injections may have extended into neighboring areas. Few brains with labeled neurons in contralateral OB or orbitofrontal cortex, which indicates that injections were not limited to the OB, were excluded from the analysis. As a side note, we observed mCherry expression in OB mitral cells and granule cells during development indicating expression of CaMKII $\alpha$  in both cell types, similar to other studies (Liu, 2000; Shani-Narkiss et al., 2020), but in contrast to a study reporting that only granule cells in OB would express CaMKII $\alpha$  (Zou et al., 2002).

Brain slices were visually inspected in a fluorescence microscope for mCherry expression. Expression was found in an age-dependent manner bilaterally in AON and nLOT, and ipsilaterally in PIR, CoA, LEC, and CA1 of the ventral hippocampus (vCA1) (Figure 1D). As previously reported, no OB-projecting neurons were found in the olfactory tubercle

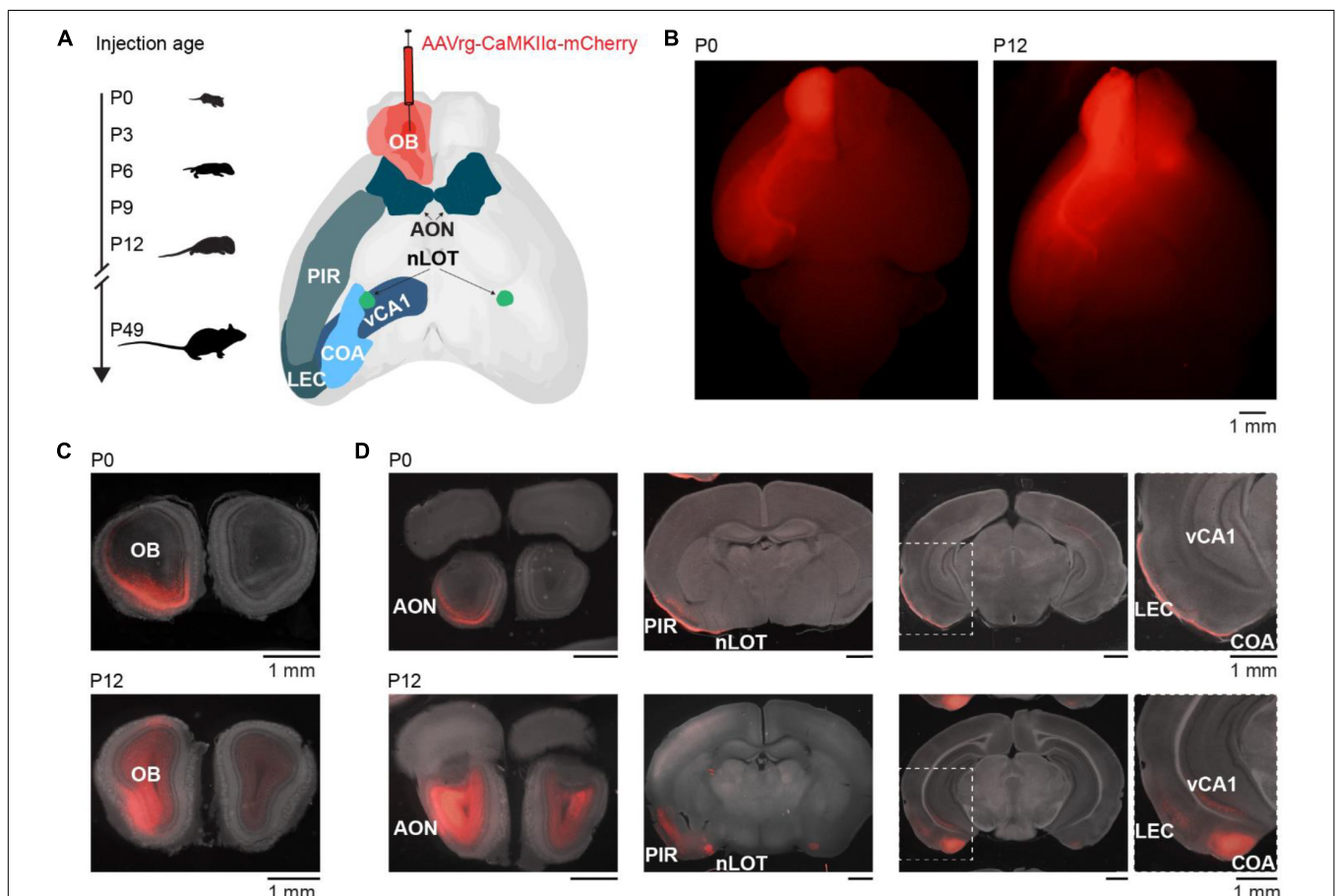
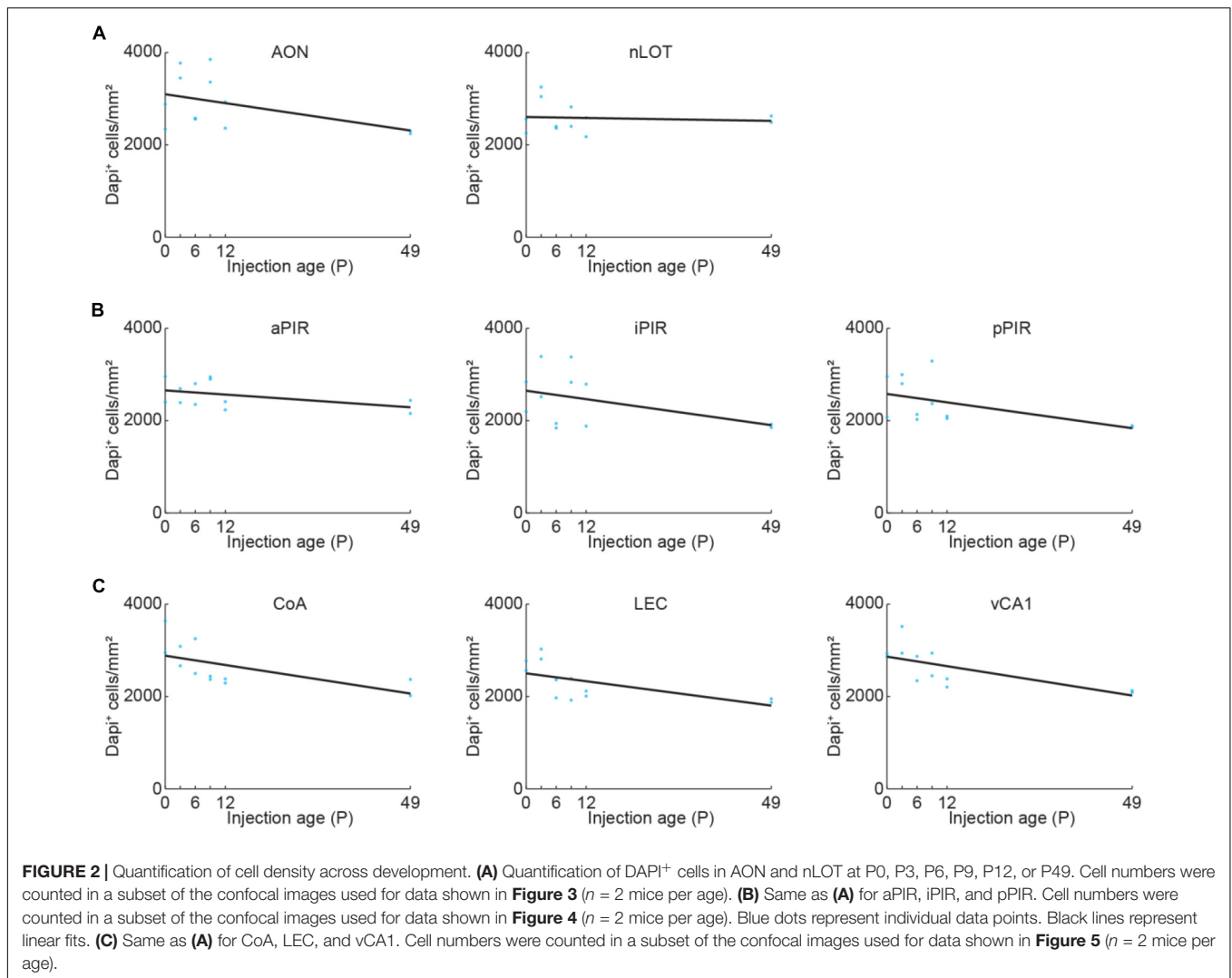


**FIGURE 1 |** Retrograde tracing to investigate the development of centrifugal projections to the OB. **(A)** Schematic diagram illustrating the investigation of glutamatergic centrifugal projections to the OB across development. Mice were injected with the retrograde virus AAVrg-CaMKII $\alpha$ -mCherry into the right OB at P0, P3, P6, P9, P12, or P49 and perfused 9 days after injection. **(B)** Representative whole-brain fluorescence images from ventral view of mCherry expression in OB and retrogradely labeled neurons for unilateral OB injections at P0 and P12. **(C)** Representative fluorescence images of mCherry expression in coronal OB slices at the injection site for OB injections at P0 and P12. **(D)** Representative fluorescence images of retrogradely labeled mCherry expression in AON, nLOT, PIR, CoA, LEC, and vCA1 for mice shown in panel **(C)**.



(In 't Zandt et al., 2019). Of note, CaMKII $\alpha$  is mainly expressed in glutamatergic neurons, thus neuromodulatory inputs to the OB were not considered in this study, but have been described in adults (Brunert and Rothermel, 2021).

General cell density might change in an area-specific manner during development. We quantified DAPI-labeled cell bodies in OB-projecting areas to be able to disentangle developmental changes of general cell density and density of OB-projecting neurons. The density of DAPI-labeled cell bodies was stable for nLOT and slightly decreased with age for all the other areas (**Figure 2** and **Supplementary Table 1**).

## Development of Olfactory Bulb-Projecting Neurons in Bilateral Anterior Olfactory Nucleus and Nucleus of the Lateral Olfactory Tract

We took confocal images from retrogradely labeled areas and mCherry expressing cells were counted automatically in images with a size of  $319.5 \times 319.5 \mu\text{m}$  with Cellpose

(Stringer et al., 2021) followed by visual confirmation (**Figure 3A**). Automatic detection worked equally well for the different ages. Similar to the adult brain, bilateral projections from AON and nLOT to the OB were found during development (**Figure 3B**). OB-projecting neurons in AON were present already at birth at low numbers and gradually increased in number with age [one-way ANOVA, ipsilateral:  $F_{(5,16)} = 16.8$ ,  $p = 7.3e^{-6}$ , contralateral:  $F_{(5,16)} = 6.2$ ,  $p = 0.002$ ] (**Figure 3C**). At P12, numbers of OB-projecting neurons had already reached 72 and 58% of adult (P49) levels for ipsilateral and contralateral AON, respectively (**Figure 3D**). Similar numbers of OB-projecting neurons were found in ipsilateral and contralateral AON from P0 to P9 but were higher for ipsilateral AON at older age.

Anterior olfactory nucleus is very close to OB, so we investigated if centrifugal projections from the more posterior nLOT are also present at birth. Similar to AON, centrifugal projections from ipsilateral nLOT were present at birth and increased gradually with age [one-way ANOVA, ipsilateral:  $F_{(5,16)} = 11.1$ ,  $p = 9.7e^{-5}$ , contralateral:  $F_{(5,16)} = 6.1$ ,  $p = 0.002$ ]

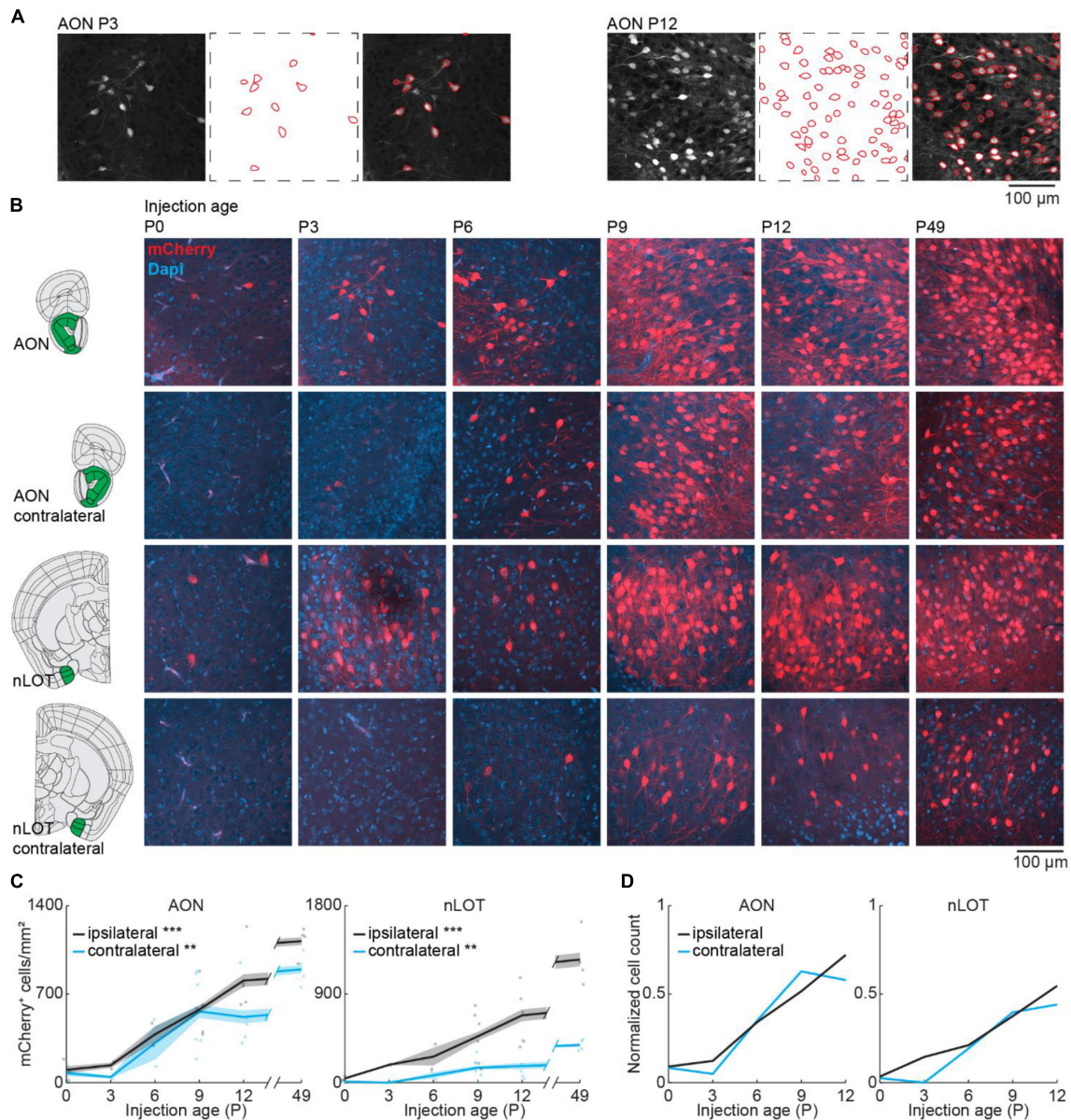


**FIGURE 3** | Bilateral centrifugal projections to olfactory bulb from AON and nLOT. **(A)** Representative confocal images detected cell outlines (red), and their overlay image for AON after OB injection at P3 and P12. **(B)** Representative confocal images of retrogradely labeled cells in ipsilateral and contralateral AON and nLOT after injection of retrograde virus into the right OB at P0, P3, P6, P9, P12, or P49. Reference images are from the Allen brain reference atlas for adult mice (Lein et al., 2007). **(C)** Quantification of retrogradely labeled cells in ipsilateral and contralateral AON and nLOT across development. **(D)** Average number of retrogradely labeled cells in ipsilateral and contralateral AON and nLOT across development normalized to adult levels at P49. Asterisks indicate significance ( $p < 0.05^*$ ,  $p < 0.01^{**}$ ,  $p < 0.001^{***}$ ).

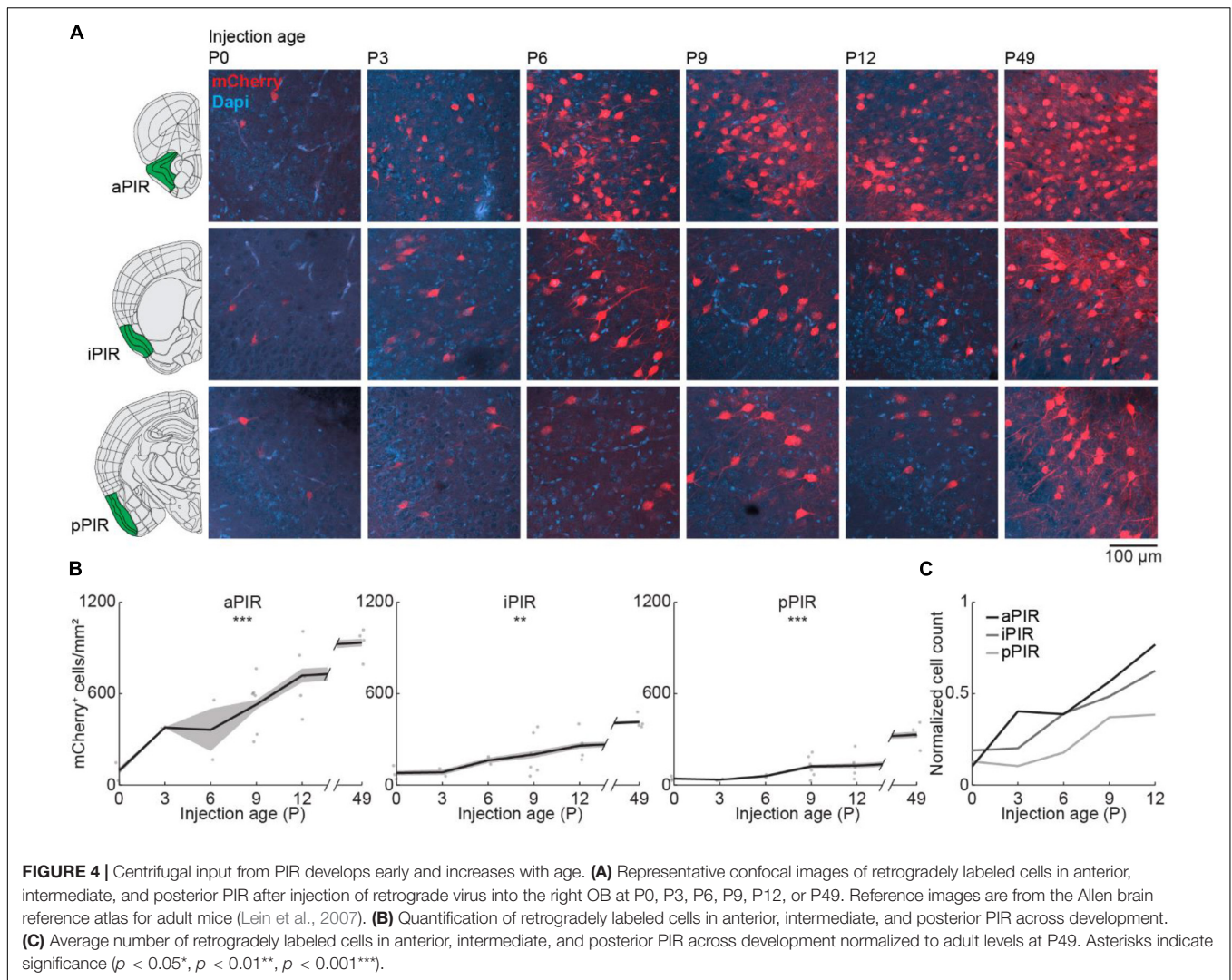
(Figure 3C and Supplementary Table 2). However, the number of centrifugal projection neurons in contralateral nLOT was lower and developed later, starting to be reliably detected at P6. Compared to adult mice, the numbers of OB-projecting neurons at P12 in ipsilateral and contralateral nLOT were at 55 and 44%, respectively.

The number of DAPI-labeled cell bodies decreased in AON and was stable in nLOT across the same developmental period (Figure 2A and Supplementary Table 1). Therefore, the change

of OB-projecting neurons cannot be explained by a change in cell numbers across development.

### Gradual Development of Olfactory Bulb Feedback Projections From Piriform Cortex

Next, we looked at the development of centrifugal projections from the ipsilateral PIR to the OB. The PIR stretches

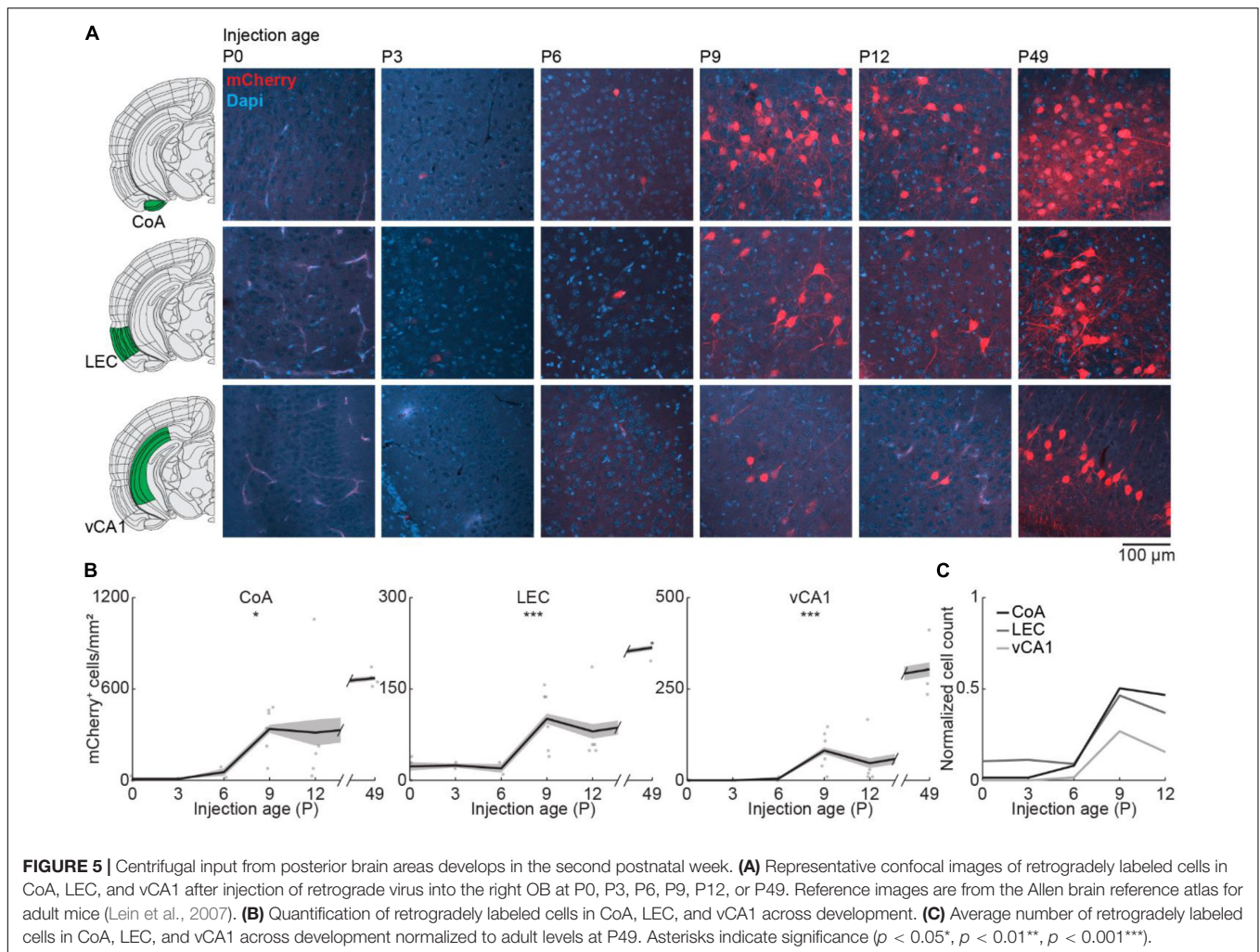


over a substantial part of the brain in anterior-posterior position. To cover the full extent of PIR, we quantified the number of OB-projecting neurons in the anterior (aPIR), intermediate (iPIR), and posterior (pPIR) part of the PIR (Figure 4A). Across development, we saw an anterior-posterior gradient in the number of labeled neurons with most OB-projecting neurons in the anterior part of PIR (Figure 4B). This gradient persisted into adulthood (P49). However, already at birth, we found OB-projecting neurons in all three parts of the PIR, and the numbers of labeled neurons gradually increased with age in all three parts [one-way ANOVA, aPIR:  $F_{(5,16)} = 9.9$ ,  $p = 0.0002$ , iPIR:  $F_{(5,16)} = 6.2$ ,  $p = 0.002$ , pPIR:  $F_{(5,16)} = 9.5$ ,  $p = 0.0002$ ] (Supplementary Table 2). At P12 numbers of OB-projecting neurons in aPIR were already at 77% of adult levels, but only at 62% for iPIR and 39% for pPIR (Figure 4C). Thus, centrifugal projections to the OB from more anterior parts of the PIR are not only higher in numbers but also develop earlier compared to more posterior parts. In contrast to OB-projecting neurons, the number of DAPI-labeled cell

bodies was similar for aPIR, iPIR, and pPIR and decreased across the same developmental period (Figure 2B and Supplementary Table 1).

### Abrupt Increase in Olfactory Bulb-Projecting Neurons in Posterior Brain Areas From P6 to P9

Finally, we looked at centrifugal inputs to OB from more posterior areas CoA, LEC, and vCA1, previously described to send ipsilateral projections to the OB in adult mice (Padmanabhan et al., 2019; Figure 5A). At birth, OB-projecting neurons were absent from CoA and vCA1, and very few neurons were labeled in LEC (Figure 5B). Numbers of labeled neurons stayed absent/low during the first postnatal week but suddenly increased from P6 to P9 for all three areas [one-way ANOVA, CoA:  $F_{(5,16)} = 4.1$ ,  $p = 0.013$ , LEC:  $F_{(5,16)} = 11.2$ ,  $p = 9.1e^{-5}$ , vCA1:  $F_{(5,16)} = 15.7$ ,  $p = 1.1e^{-5}$ ] (Supplementary Table 2). The numbers of OB-projecting neurons in CoA were higher than in LEC and vCA1 at all ages investigated. At P12, numbers of OB-projecting



neurons were at 47% of adult levels (P49) for CoA and at 37% for LEC, but only at 15% for vCA1, indicating a late development of centrifugal projections from vCA1 to OB (Figure 5C). The number of DAPI-labeled cell bodies was similar for CoA, LEC, and vCA1 and decreased across the same developmental period (Figure 2C and Supplementary Table 1).

### Consistent Area-Specific Development of Olfactory Bulb-Feedback Projections With a Different Retrograde Tracer

We used a retrograde virus to express mCherry in OB-projecting neurons under the control of the CaMKII $\alpha$  promoter. CaMKII $\alpha$  is expressed at birth, but the expression increases in some brain areas during postnatal development (Gou et al., 2020). To test, if the developmental increase in OB-projecting neurons is influenced by the strength of CaMKII $\alpha$  expression, we used a second method of retrograde labeling that is independent of gene expression. For this, we injected red-fluorescent Retrobeads into the OB at P0 ( $n = 2$ ), P6 ( $n = 2$ ), or P12 ( $n = 2$ ) and quantified the intensity of retrograde labeling in the same areas as above.

Tracing with Retrobeads yielded similar results to viral tracing for all investigated brain areas (Figure 6).

## DISCUSSION

We performed retrograde virus-labeling across development to describe the formation of centrifugal projections to the OB. We found that centrifugal inputs from AON, nLOT, and PIR are already present at birth, but increase extensively in a gradual manner during postnatal development. Contralateral inputs from AON were present at birth, but were not detected before P6 for nLOT. Centrifugal inputs from PIR develop in an anterior-posterior gradient with OB-projecting neurons from anterior parts developing earlier and reaching higher numbers. Centrifugal inputs from CoA and vCA1 only started to be detected at P6 whereas few retrogradely labeled neurons were present at birth in LEC. The development of OB-projecting neurons in areas related to emotional and memory processing such as CoA, vCA1, and LEC was characterized by a sudden increase at the start of the second postnatal week. While neurons are still migrating into superficial layers of the neocortex

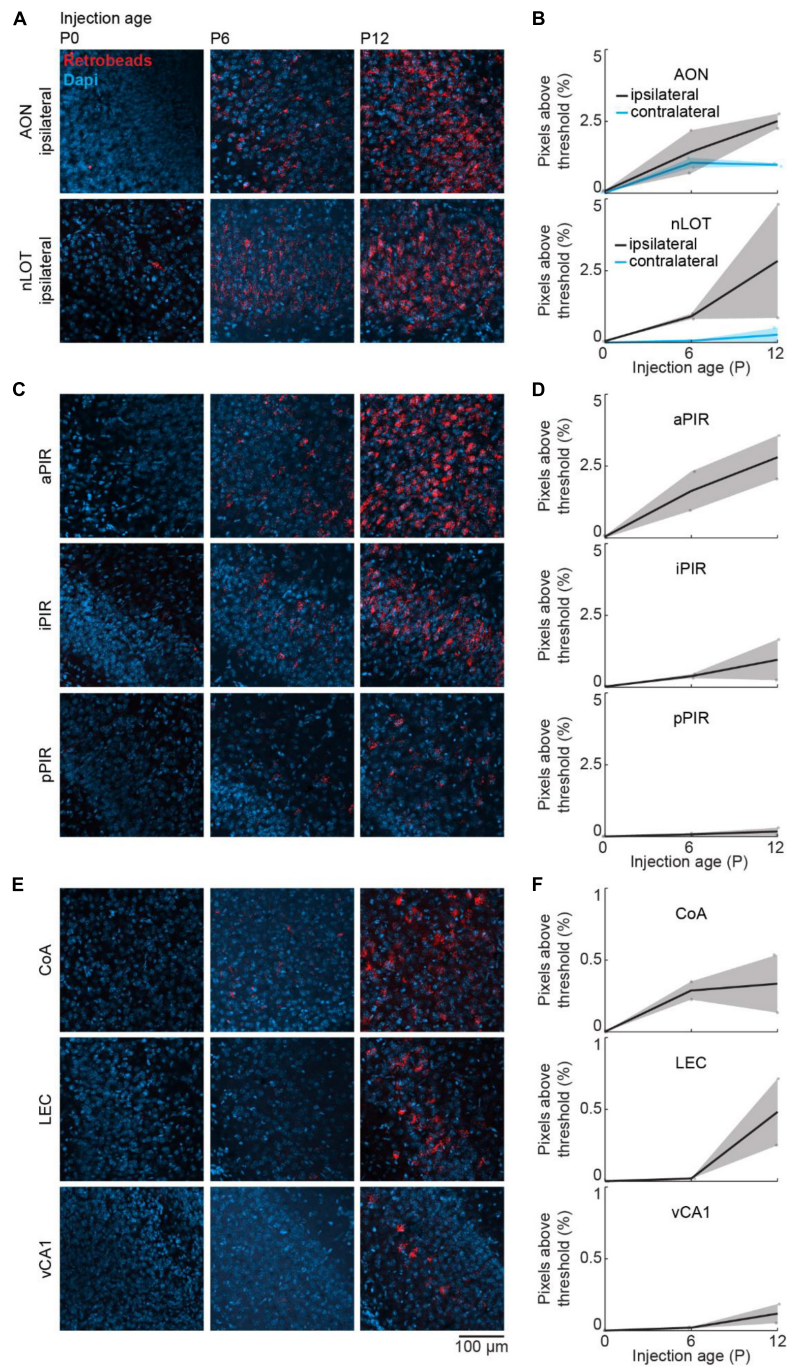


**FIGURE 6** | Retrograde tracing to investigate the development of centrifugal projections to the OB using Retrobeads. **(A)** Representative confocal images of retrogradely labeled cells in ipsilateral AON and nLOT after injection of red Retrobeads into the right OB at P0, P6, or P12 ( $n = 2$  mice per age). **(B)** Quantification of fluorescent pixels above threshold in the red channel in ipsilateral and contralateral AON and nLOT across development. **(C)** Same as **(A)** for aPIR, iPIR, and pPIR. **(D)** Same as **(B)** for aPIR, iPIR, and pPIR. **(E)** Same as **(A)** for CoA, LEC, and vCA1. **(F)** Same as **(B)** for CoA, LEC, and vCA1.

until P4 in mice, excitatory neurons in the allocortex, such as PIR, have reached their final position at birth (Klingler, 2017; Kast and Levitt, 2019). This is consistent with our analysis of DAPI<sup>+</sup> labeled cell bodies across age and indicates that the developmental increase of OB-projecting neurons is not due to

increased cell density. Therefore, we hypothesize that the increase of retrogradely labeled neurons during postnatal development reflects the late arrival of centrifugal axons in the OB, similar to the postnatal formation of callosal axons in somatosensory cortex (Zhou et al., 2021). Similarly, feedback projections in

the rodent visual system develop during the second postnatal week, whereas feedforward projections are present at birth (Dong et al., 2004; Berezovskii et al., 2011) and thalamocortical axons are established prenatally, but corticothalamic projections only reach the thalamus postnatally (Grant et al., 2012). The delayed detection of OB-projecting neurons in more posterior areas may arise from the longer distance to the OB. The early maturation of PIR in contrast to other cortical areas might further contribute to the earlier formation of centrifugal inputs in comparison to LEC and vCA1. It is unknown to what extent molecular cues and activity-dependent mechanisms that influence axon growth contribute to the different time courses in the formation of OB-projections from different areas.

Viral injections of the same volume and concentration were used for all age groups, despite the change in brain size, and may have resulted in a smaller relative injection area in the OB for older age groups. We expected to see an increase of retrogradely labeled neurons with age and therefore decided to keep injection parameters constant to make sure that increases with age are not artificially induced by adapting injection volumes to brain size. Thus, the actual age-related increase of OB-projecting neurons seen for all areas may be slightly underestimated. A decrease of cellular density with age shown by staining for DAPI, presumably due to more space taken up by dendrites and axons, might further contribute to this effect.

Further, we found similar developmental trajectories using Retrobeads as a different retrograde labeling strategy, independent of gene expression. The beads consist of hydrophobic latex microspheres that tend to stick to cell membranes and accumulate after retrograde diffusion to the soma (Katz et al., 1984). This confirms that the observed developmental increase of neurons projecting to the OB and the area-specific differences do not depend on gene expression or synaptic maturation.

In the adult brain, the OB also receives inputs from neuromodulatory areas, such as noradrenergic input from the locus coeruleus, serotonergic input from the raphe nuclei, and cholinergic input from the basal forebrain (Brunert and Rothermel, 2021). These inputs have been implicated in the modulation of odor discrimination and odor learning. While noradrenergic inputs are well developed at birth in rodents (McLean and Shipley, 1991), serotonergic and cholinergic inputs mainly form postnatally (McLean and Shipley, 1987; Le Jeune and Jourdan, 1991), similar to what we report for glutamatergic inputs.

Olfactory information is processed in two stages in the OB: at the glomerular level, where local interneurons mediate inhibition within and between glomeruli and through lateral and recurrent inhibition of mitral and tufted cells by inhibitory interneurons such as granule cells in the external plexiform layer (Nagayama et al., 2014). Centrifugal inputs to the OB mainly target inhibitory neurons in the glomerular and granule cell layer of the OB but have only weak direct inputs onto mitral cells (Boyd et al., 2012; Markopoulos et al., 2012). Thereby, centrifugal inputs to OB are ideally positioned to modulate olfactory processing and coordinated network activity in the olfactory system. Interestingly, the generation and maturation of

inhibitory neurons in OB extends well into the postnatal period (Batista-Brito et al., 2008).

In adult rodents, coherent beta oscillations between OB and brain areas such as PIR, LEC, hippocampus, and prefrontal cortex have been implicated in memory processing and decision making (Martin et al., 2006, 2007; Igarashi et al., 2014; Symanski et al., 2021). Interestingly, the generation of beta oscillations in OB has been shown to depend on centrifugal inputs (Neville and Haberly, 2003; Ravel et al., 2003). Previous studies have shown that neuronal activity in OB drives oscillatory activity in the beta frequency range in LEC, hippocampus, and prefrontal cortex already at the beginning of the second postnatal week (Kostka and Hanganu-Opatz, 2021). Considering the emergence of feedback projections to the OB from memory-related brain areas around the same time period suggests that already at this age past experience could shape sensory processing. The area-specific development of centrifugal projections to the OB suggests that top-down modulation changes with age. We show that feedback from early olfactory areas, such as AON and aPIR, develops first and presumably contributes to basic sensory processing already shortly after birth. In contrast, the delayed maturation of feedback from higher brain areas, such as CoA, LEC and vHP, suggests that valence and memory dependent modulation of OB activity only emerges later in life. Further research is required to understand the functional role of area-specific centrifugal inputs for olfactory processing during neonatal development.

## DATA AVAILABILITY STATEMENT

The raw data supporting the conclusions of this article will be made available by the authors, without undue reservation.

## ETHICS STATEMENT

The animal study was reviewed and approved by the Behörde für Gesundheit und Verbraucherschutz Hamburg ID 15/17.

## AUTHOR CONTRIBUTIONS

JK and SHB designed the study and performed the experiments, analyzed the data, and interpreted the data and wrote the manuscript. Both authors contributed to the article and approved the submitted version.

## FUNDING

This work was funded by grants of the European Research Council (ERC-2015-CoG 681577 to Ileana L. Hanganu-Opatz) and the German Research Foundation (Ha4466/11-1 and 178316478 – B5 to Ileana L. Hanganu-Opatz). SHB is a WBP Fellow (German Research Foundation) – 445900988.

## ACKNOWLEDGMENTS

We thank Ileana L. Hanganu-Opatz for conceptual and financial support. We also thank A. M. Thies, A. Marquardt, P. Putthoff, and A. Dahlmann for excellent technical assistance.

## REFERENCES

- Batista-Brito, R., Close, J., Machold, R., and Fishell, G. (2008). The distinct temporal origins of olfactory bulb interneuron subtypes. *J. Neurosci.* 28, 3966–3975. doi: 10.1523/JNEUROSCI.5625-07.2008
- Berezovskii, V. K., Nassi, J. J., and Born, R. T. (2011). Segregation of feedforward and feedback projections in mouse visual cortex. *J. Comp. Neurol.* 519, 3672–3683. doi: 10.1002/cne.22675
- Boyd, A. M., Kato, H. K., Komiyama, T., and Isaacson, J. S. (2015). Broadcasting of cortical activity to the olfactory bulb. *Cell Rep.* 10, 1032–1039. doi: 10.1016/j.celrep.2015.01.047
- Boyd, A. M., Sturgill, J. F., Poo, C., and Isaacson, J. S. (2012). Cortical feedback control of olfactory bulb circuits. *Neuron* 76, 1161–1174. doi: 10.1016/j.neuron.2012.10.020
- Brunert, D., and Rothmel, M. (2021). Extrinsic neuromodulation in the rodent olfactory bulb. *Cell Tissue Res.* 383, 507–524. doi: 10.1007/s00441-020-03365-9
- Dong, H., Wang, Q., Valkova, K., Gonchar, Y., and Burkhalter, A. (2004). Experience-dependent development of feedforward and feedback circuits between lower and higher areas of mouse visual cortex. *Vis. Res.* 44, 3389–3400. doi: 10.1016/j.visres.2004.09.007
- Gao, Y., and Strowbridge, B. W. (2009). Long-term plasticity of excitatory inputs to granule cells in the rat olfactory bulb. *Nat. Neurosci.* 12, 731–733. doi: 10.1038/nn.2319
- Gilbert, C. D., and Sigman, M. (2007). Brain states: top-down influences in sensory processing. *Neuron* 54, 677–696. doi: 10.1016/j.neuron.2007.05.019
- Gou, G., Roca-Fernandez, A., Kilinc, M., Serrano, E., Reig-Viader, R., Araki, Y., et al. (2020). SynGAP splice variants display heterogeneous spatio-temporal expression and subcellular distribution in the developing mammalian brain. *J. Neurochem.* 154, 618–634. doi: 10.1111/jnc.14988
- Grant, E., Hoerder-Suabedissen, A., and Molnar, Z. (2012). Development of the corticothalamic projections. *Front. Neurosci.* 6:53. doi: 10.3389/fnins.2012.00053
- Gretenkord, S., Kostka, J. K., Hartung, H., Watznauer, K., Fleck, D., Minier-Toribio, A., et al. (2019). Coordinated electrical activity in the olfactory bulb gates the oscillatory entrainment of entorhinal networks in neonatal mice. *PLoS Biol.* 17:e2006994. doi: 10.1371/journal.pbio.2006994
- Igarashi, K. M., Ieki, N., An, M., Yamaguchi, Y., Nagayama, S., Kobayakawa, K., et al. (2012). Parallel mitral and tufted cell pathways route distinct odor information to different targets in the olfactory cortex. *J. Neurosci.* 32, 7970–7985. doi: 10.1523/JNEUROSCI.0154-12.2012
- Igarashi, K. M., Lu, L., Colgin, L. L., Moser, M.-B., and Moser, E. I. (2014). Coordination of entorhinal-hippocampal ensemble activity during associative learning. *Nature* 510, 143–147. doi: 10.1038/nature13162
- In 't Zandt, E. E., Cansler, H. L., Denson, H. B., and Wesson, D. W. (2019). Centrifugal innervation of the olfactory bulb: a reappraisal. *eNeuro* 6:ENEURO.0390-18.2019. doi: 10.1523/ENEURO.0390-18.2019
- Kast, R. J., and Levitt, P. (2019). Precision in the development of neocortical architecture: from progenitors to cortical networks. *Prog. Neurobiol.* 175, 77–95. doi: 10.1016/j.pneurobio.2019.01.003
- Katz, L. C., Burkhalter, A., and Dreyer, W. J. (1984). Fluorescent latex microspheres as a retrograde neuronal marker for in vivo and in vitro studies of visual cortex. *Nature* 310, 498–500. doi: 10.1038/310498a0
- Kiselycznyk, C. L., Zhang, S., and Linster, C. (2006). Role of centrifugal projections to the olfactory bulb in olfactory processing. *Learn. Mem.* 13, 575–579. doi: 10.1101/lm.285706
- Klingler, E. (2017). Development and organization of the evolutionarily conserved three-layered olfactory cortex. *eNeuro* 4:ENEURO.0193-16.2016. doi: 10.1523/ENEURO.0193-16.2016
- Kostka, J. K., Gretenkord, S., Spehr, M., and Hanganu-Opatz, I. L. (2020). Bursting mitral cells time the oscillatory coupling between olfactory bulb and entorhinal networks in neonatal mice. *J. Physiol.* 598, 5753–5769. doi: 10.1113/JP280131
- Kostka, J. K., and Hanganu-Opatz, I. L. (2021). Olfactory-driven beta band entrainment of limbic circuitry during neonatal development. *bioRxiv* [Preprint]. doi: 10.1101/2021.10.04.463041
- Le Jeune, H., and Jourdan, F. (1991). Postnatal development of cholinergic markers in the rat olfactory bulb: a histochemical and immunocytochemical study. *J. Comp. Neurol.* 314, 383–395. doi: 10.1002/cne.903140212
- Lein, E. S., Hawrylycz, M. J., Ao, N., Ayres, M., Bensinger, A., Bernard, A., et al. (2007). Genome-wide atlas of gene expression in the adult mouse brain. *Nature* 445, 168–176. doi: 10.1038/nature05453
- Liu, N. (2000). Regional distribution of protein kinases in normal and odor-deprived mouse olfactory bulbs. *Chem. Senses* 25, 401–406. doi: 10.1093/chemse/25.4.401
- Logan, D. W., Brunet, L. J., Webb, W. R., Cutforth, T., Ngai, J., and Stowers, L. (2012). Learned recognition of maternal signature odors mediates the first suckling episode in mice. *Curr. Biol.* 22, 1998–2007. doi: 10.1016/j.cub.2012.08.041
- Luskin, M. B., and Price, J. L. (1983). The topographic organization of associational fibers of the olfactory system in the rat, including centrifugal fibers to the olfactory bulb. *J. Compar. Neurol.* 216, 264–291. doi: 10.1002/cne.902160305
- Markopoulos, F., Rokni, D., Gire, D. H., and Murthy, V. N. (2012). Functional properties of cortical feedback projections to the olfactory bulb. *Neuron* 76, 1175–1188. doi: 10.1016/j.neuron.2012.10.028
- Martin, C., Beshele, J., and Kay, L. M. (2007). An olfacto-hippocampal network is dynamically involved in odor-discrimination learning. *J. Neurophysiol.* 98, 2196–2205. doi: 10.1152/jn.00524.2007
- Martin, C., Gervais, R., Messaoudi, B., and Ravel, N. (2006). Learning-induced oscillatory activities correlated to odour recognition: a network activity. *Eur. J. Neurosci.* 23, 1801–1810. doi: 10.1111/j.1460-9568.2006.04711.x
- McLean, J. H., and Shipley, M. T. (1987). Serotonergic afferents to the rat olfactory bulb: II. Changes in fiber distribution during development. *J. Neurosci.* 7, 3029–3039. doi: 10.1523/JNEUROSCI.07-10-03029.1987
- McLean, J. H., and Shipley, M. T. (1991). Postnatal development of the noradrenergic projection from locus coeruleus to the olfactory bulb in the rat. *J. Compar. Neurol.* 304, 467–477. doi: 10.1002/cne.903040310
- Nagayama, S., Homma, R., and Imamura, F. (2014). Neuronal organization of olfactory bulb circuits. *Front. Neural Circ.* 8:98. doi: 10.3389/fncir.2014.00098
- Neville, K. R., and Haberly, L. B. (2003). Beta and gamma oscillations in the olfactory system of the urethane-anesthetized rat. *J. Neurophysiol.* 90, 3921–3930. doi: 10.1152/jn.00475.2003
- Padmanabhan, K., Osakada, F., Tarabrina, A., Kizer, E., Callaway, E. M., Gage, F. H., et al. (2019). Centrifugal inputs to the main olfactory bulb revealed through whole brain circuit-mapping. *Front. Neuroanat.* 12:115. doi: 10.3389/fnana.2018.00115
- Ravel, N., Chabaud, P., Martin, C., Gaveau, V., Hugues, E., Tallon-Baudry, C., et al. (2003). Olfactory learning modifies the expression of odour-induced oscillatory responses in the gamma (60–90 Hz) and beta (15–40 Hz) bands in the rat olfactory bulb. *Eur. J. Neurosci.* 17, 350–358. doi: 10.1046/j.1460-9568.2003.02445.x
- Shani-Narkiss, H., Vinograd, A., Landau, I. D., Tasaka, G., Yayon, N., Terletsky, S., et al. (2020). Young adult-born neurons improve odor coding by mitral cells. *Nat. Commun.* 11:5867. doi: 10.1038/s41467-020-19472-8

## SUPPLEMENTARY MATERIAL

The Supplementary Material for this article can be found online at: <https://www.frontiersin.org/articles/10.3389/fnins.2022.815282/full#supplementary-material>

- Shiple, M. T., and Adamek, G. D. (1984). The connections of the mouse olfactory bulb: a study using orthograde and retrograde transport of wheat germ agglutinin conjugated to horseradish peroxidase. *Brain Res. Bull.* 12, 669–688. doi: 10.1016/0361-9230(84)90148-5
- Stringer, C., Wang, T., Michaelos, M., and Pachitariu, M. (2021). Cellpose: a generalist algorithm for cellular segmentation. *Nat. Methods* 18, 100–106. doi: 10.1038/s41592-020-01018-x
- Sullivan, R. M. (2003). Developing a sense of safety: the neurobiology of neonatal attachment. *Ann. N.Y. Acad. Sci.* 1008, 122–131. doi: 10.1196/annals.1301.013
- Symanski, C. A., Bladon, J. H., Kullberg, E. T., and Jadhav, S. P. (2021). Rhythmic coordination of hippocampal-prefrontal ensembles for odour-place associative memory and decision making. *bioRxiv* [Preprint]. doi: 10.1101/2020.06.08.140939
- Walz, A., Omura, M., and Mombaerts, P. (2006). Development and topography of the lateral olfactory tract in the mouse: imaging by genetically encoded and injected fluorescent markers. *J. Neurobiol.* 66, 835–846. doi: 10.1002/neu.20266
- Zhou, J., Lin, Y., Huynh, T., Noguchi, H., Bush, J. O., and Pleasure, S. J. (2021). NMDA receptors control development of somatosensory callosal axonal projections. *eLife* 10:e59612. doi: 10.7554/eLife.59612
- Zou, D.-J., Greer, C. A., and Firestein, S. (2002). Expression pattern of  $\alpha$ CaMKII in the mouse main olfactory bulb. *J. Compar. Neurol.* 443, 226–236. doi: 10.1002/cne.10125

**Conflict of Interest:** The authors declare that the research was conducted in the absence of any commercial or financial relationships that could be construed as a potential conflict of interest.

**Publisher's Note:** All claims expressed in this article are solely those of the authors and do not necessarily represent those of their affiliated organizations, or those of the publisher, the editors and the reviewers. Any product that may be evaluated in this article, or claim that may be made by its manufacturer, is not guaranteed or endorsed by the publisher.

Copyright © 2022 Kostka and Bitzenhofer. This is an open-access article distributed under the terms of the Creative Commons Attribution License (CC BY). The use, distribution or reproduction in other forums is permitted, provided the original author(s) and the copyright owner(s) are credited and that the original publication in this journal is cited, in accordance with accepted academic practice. No use, distribution or reproduction is permitted which does not comply with these terms.